Supplementary Material to

"The influence of spatial distribution of leads and ice floes on the atmospheric boundary layer over fragmented sea ice"

Marta Wenta, Agnieszka Herman

Institute of Oceanography, University of Gdansk, Poland
Email:marta.wenta@phdstud.ug.edu.pl

Supplementary Table 1: Model setup parameters.

Weather Research and Forecasting Model configuration			
Model domain	Rectangular, periodic boundaries used in both horizontal directions	Model top height	2000 m
Horizontal Resolution	100 m	Number of eta levels	60
Number of grid points	200 x 200		
Physics Parametrization	**Description**	**Sea Ice Options**	
Microphysics (mp_physics)	WRF Single-Moment 5-class-scheme	fractional_seaice	Treats ice as fractional field
Longwave Radiation (ra_lw_physics)	RRTMG Scheme, an improved version of RRTM (Rapid Radiative Transfer Model) which include the MCICA (Mone-Carlo Independent Column Approximation) method of random cloud overlap	seaice_albedo_default	Default value for sea ice albedo (0.75) (Insignificant during Arctic winter)
Shortwave Radiation (ra_sw_physics)	Goddard Shortwave Scheme (insignificant during Arctic winter)	seaice_snowdepth_max	Maximum allowed accumulation of snow (m) on sea ice (1.e10)
Surface Layer (sf_sfclay_physics)	Eta Similarity Scheme: used in Eta Model	seaice_snowdepth_min	Minimum snow depth (m) on sea ice (0.001)
Land Layer (sf_surface_physics)	Noah Land Surface Model (with 4 soil layers)	seaice_thickness_default	Default value of seaice thickness (m) (1.5)
Planetary Boundary Layer (bl_pbl_physics)	No Planetary Boundary Layer parametrization		
Large-Eddy Simulation	1.5 order TKE closure		
Cumulun Parametrization	No cumulus parametrization		

Supplementary Note S1. Initial atmospheric profiles and conditions

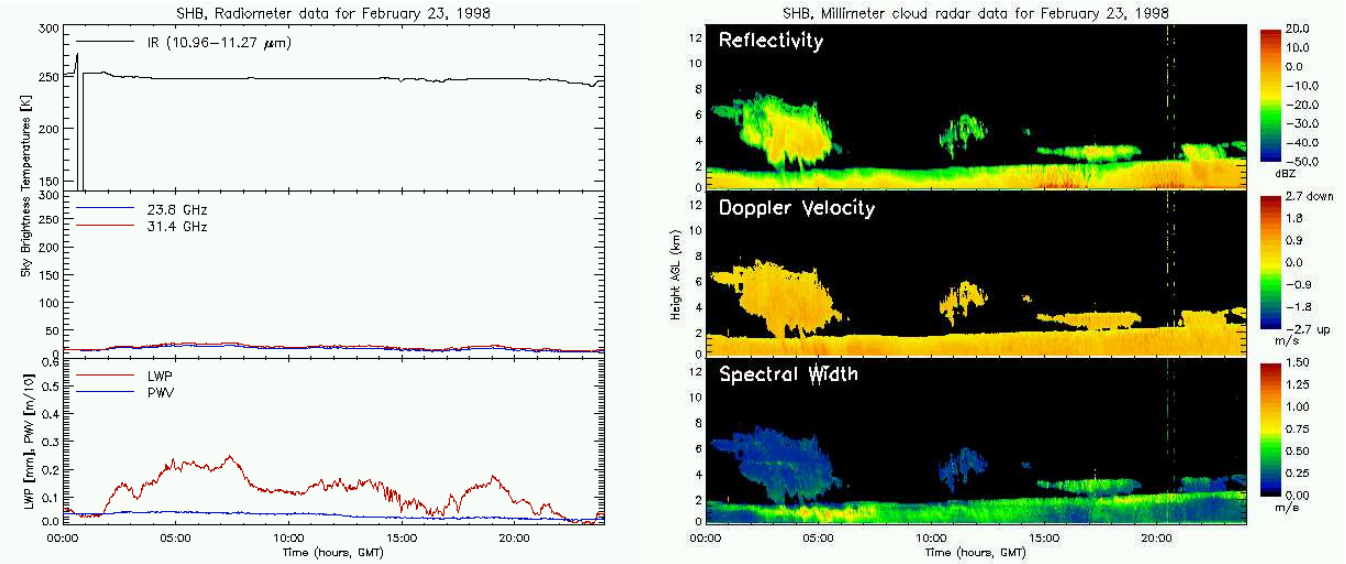

Supplementary Figure 1: Vertical profiles of radiometer cloud data (left) and cloud radar data (right) over the SHEBA station on 23. Feb. 1998. (source: Earth System research Laboratory, www.esrl.noaa.gov/psd/arctic/sheba, accessed 16 Feb 2017).

Vertical profiles of relative humidity h_r, wind speed U, potential temperature T_i, and atmospheric pressure P_i are obtained, along with surface pressure value P_s, in order to configure model idealized run (Fig. 4 in the main text). The following equations are applied to obtain required vapor mixing ratio w and altitude profiles H_i:

$$\begin{aligned} w &= \frac{621.97 \cdot e}{P_s - e} \\ e &= e_s \cdot h_r \\ e_s &= 6.11 \cdot 10^{\frac{7.5 T_i}{273.373 + T_i}} \\ H_u &= \frac{\frac{P_s}{P_i}((\frac{1}{5.257} - 1) \cdot T_i)}{0.0065} \end{aligned} \tag{1}$$

Supplementary Note S2. Sea ice distribution maps

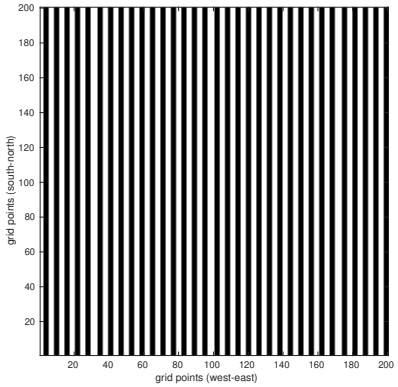

(a)

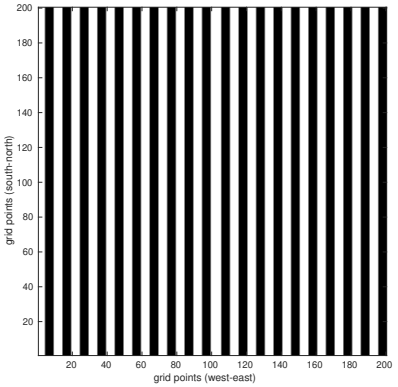

(b)

Supplementary Figure 2: Sea ice map for ice concentration $c = 50\%$, number of leads $N_l = 33$ (a), $N_l = 20$ (b).

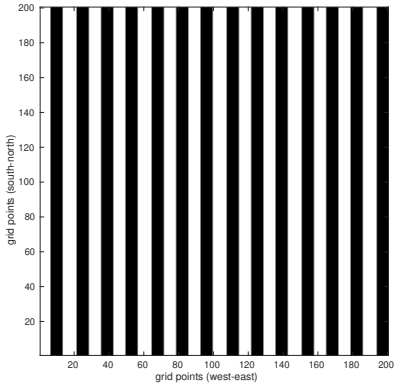

(a)

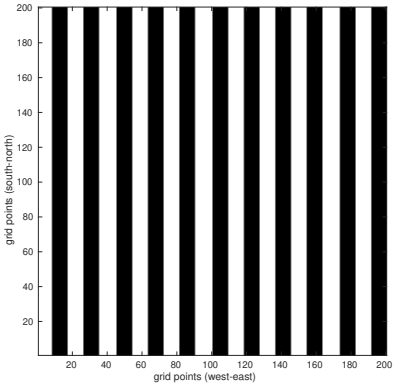

(b)

Supplementary Figure 3: Sea ice map for ice concentration $c = 50\%$, number of leads $N_l = 14$ (a), $N_l = 11$ (b).

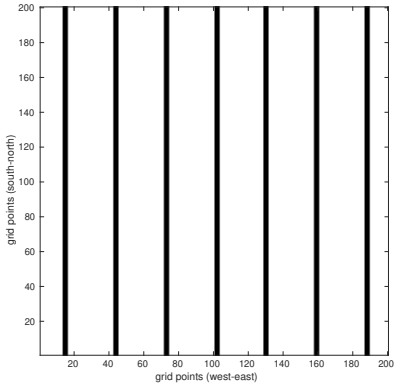

(a)

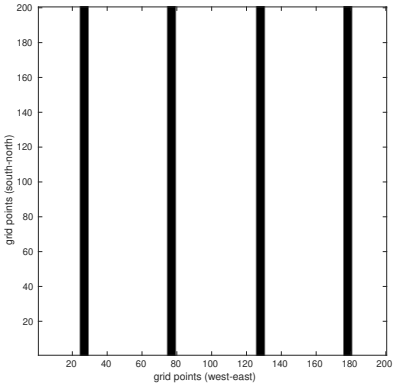

(b)

Supplementary Figure 4: Sea ice map for ice concentration $c = 90\%$, number of leads $N_l = 7$ (a), $N_l = 4$ (b).

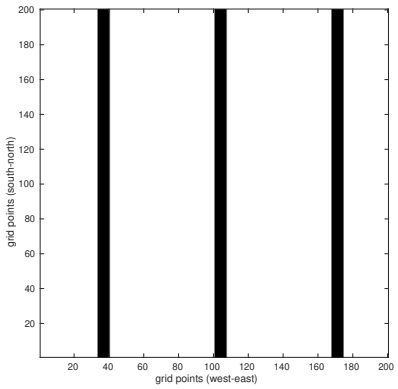

(a)

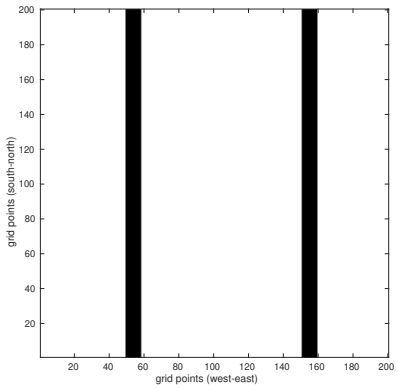

(b)

Supplementary Figure 5: Sea ice map for ice concentration $c = 90\%$, number of leads $N_l = 3$ (a), $N_l = 2$ (b).

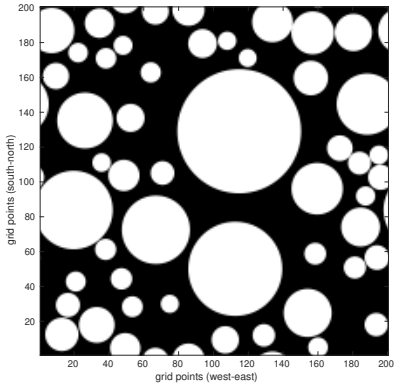

(a)

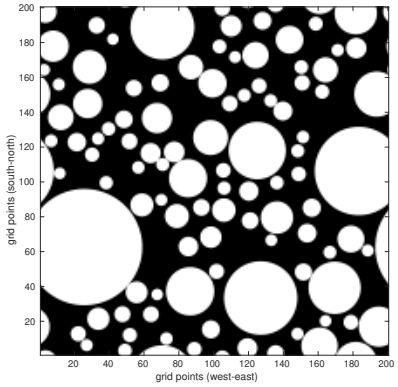

(b)

Supplementary Figure 6: Sea ice map for ice concentration $c = 50\%$, number of floes $N_f = 50$ (a), $N_f = 100$ (b).

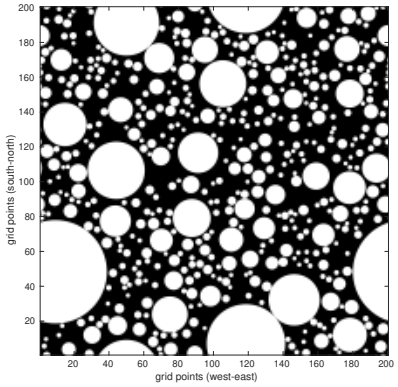

(a)

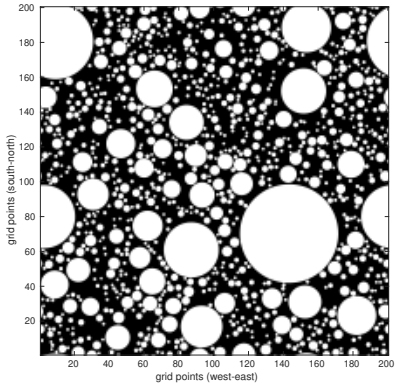

(b)

Supplementary Figure 7: Sea ice map for ice concentration $c = 50\%$, number of floes $N_f = 500$ (a), $N_f = 1000$ (b).

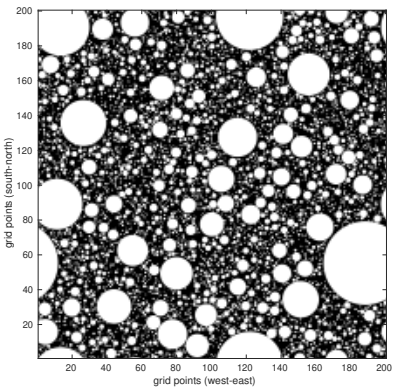

(a)

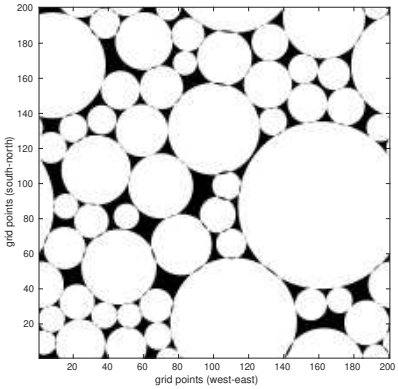

(b)

Supplementary Figure 8: Sea ice map for ice concentration $c = 50\%$, number of floes $N_f = 5000$ (a), and for ice concentration $c = 90\%$ $N_f = 50$ (b).

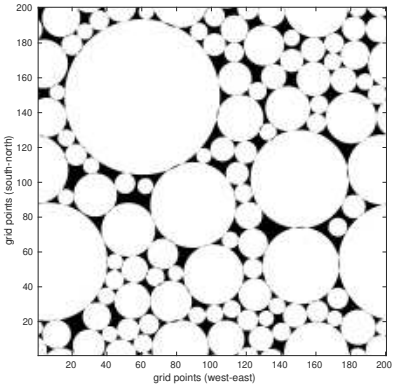

(a)

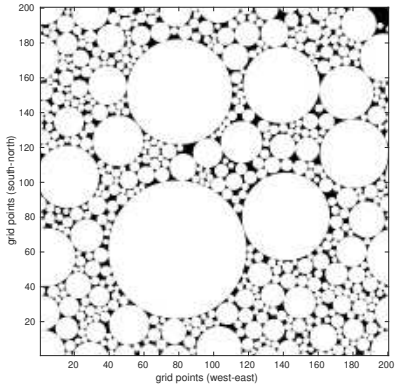

(b)

Supplementary Figure 9: Sea ice map for ice concentration $c = 90\%$, number of floes $N_f = 100$ (b), $N_f = 500$ (c).

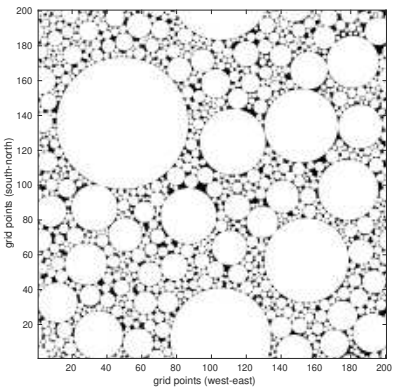

(a)

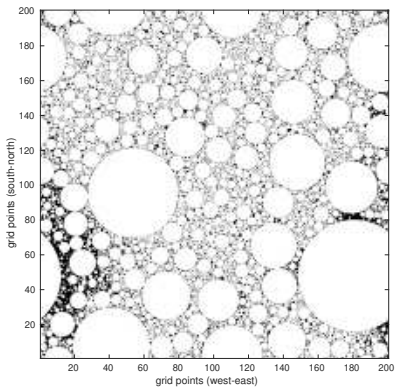

(b)

Supplementary Figure 10: Sea ice map for ice concentration $c = 90\%$, number of floes $N_f = 1000$ (a), $N_f = 5000$ (b).

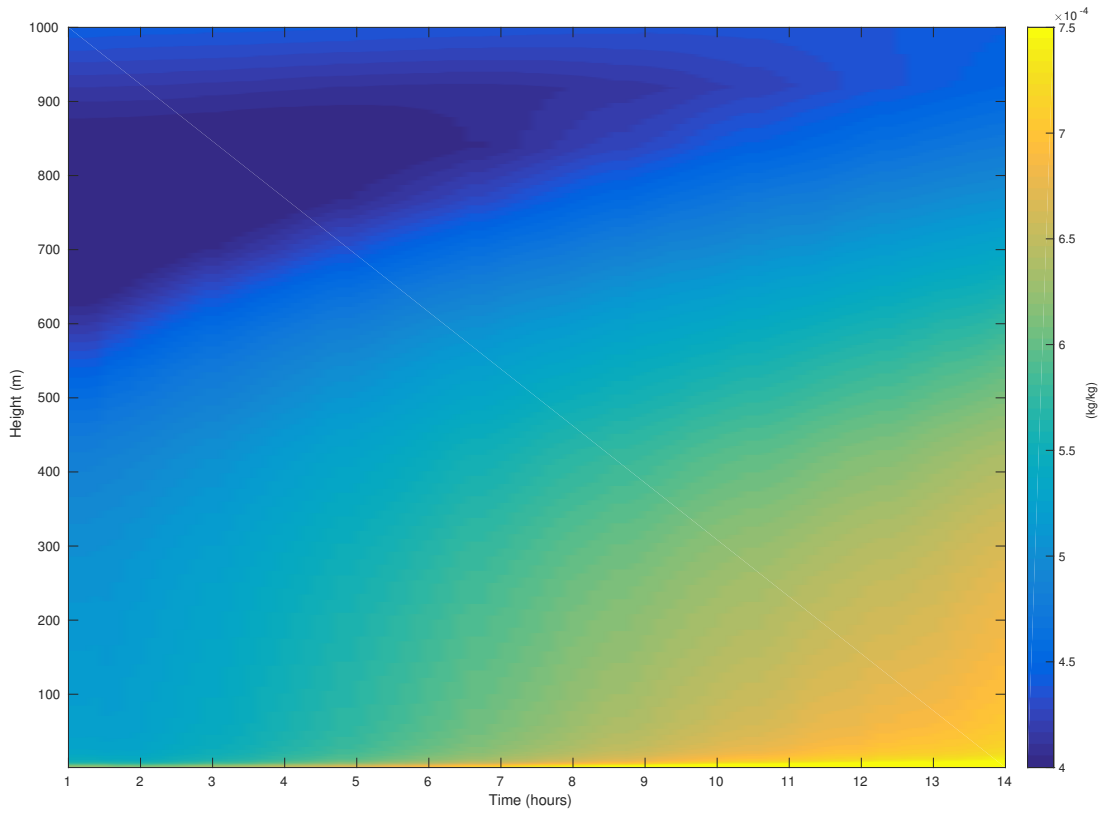

(a)

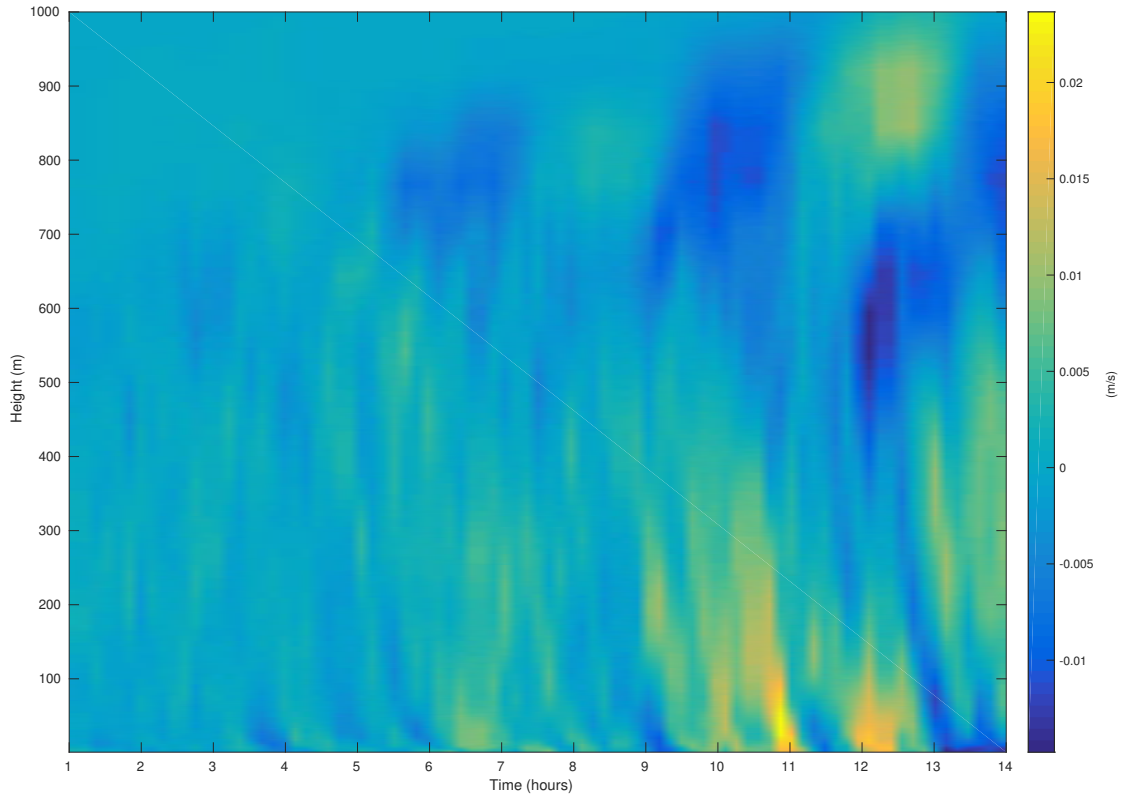

(b)

Supplementary Figure 11: Simulation initiated with zero wind speed profile, sea ice concentration $c = 50\%$ and number of leads $N_l = 20$. (a) Area averaged water vapour content. (b) Area averaged W-E wind component.

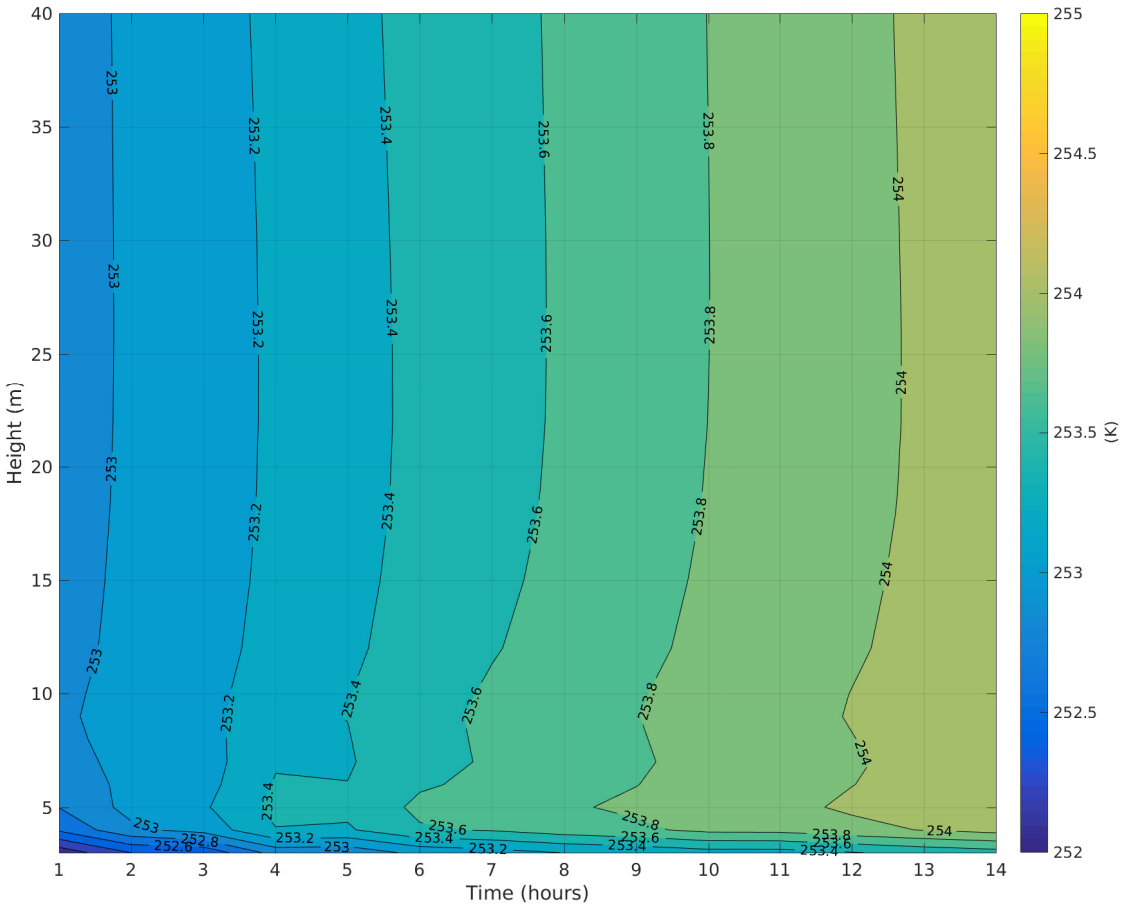

(a)

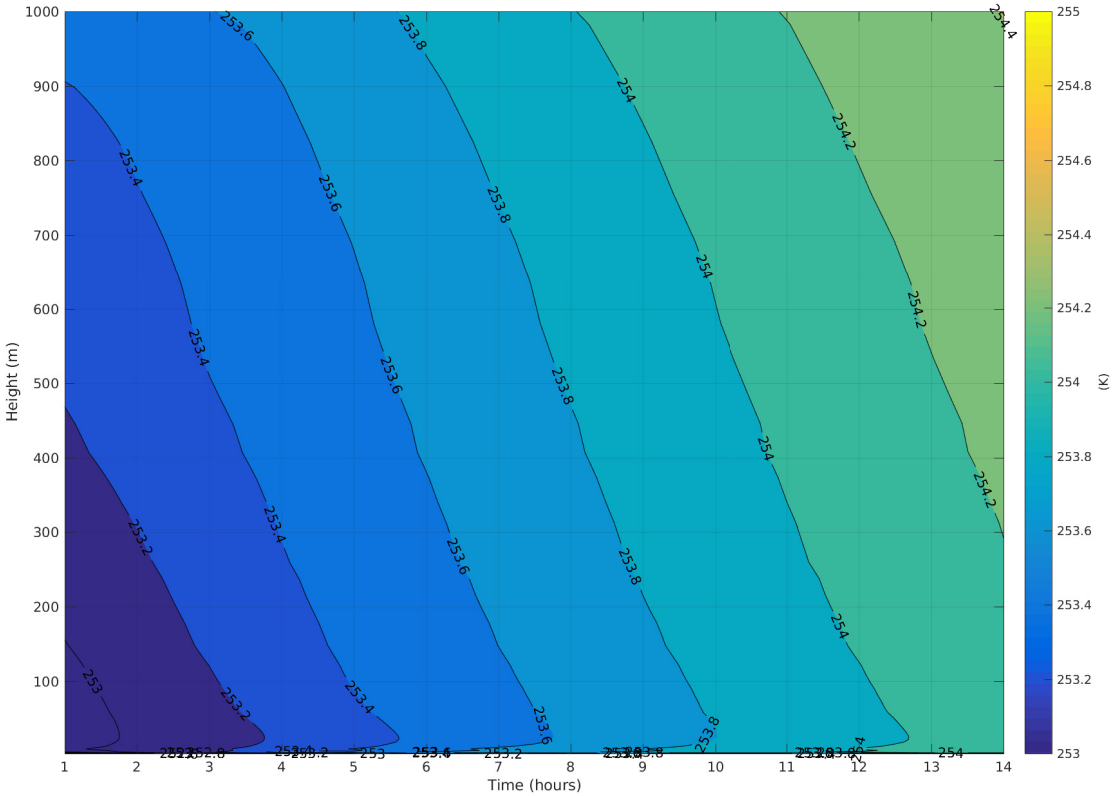

(b)

Supplementary Figure 12: As in Fig. 11, (a) and (b) Area averaged temperature.

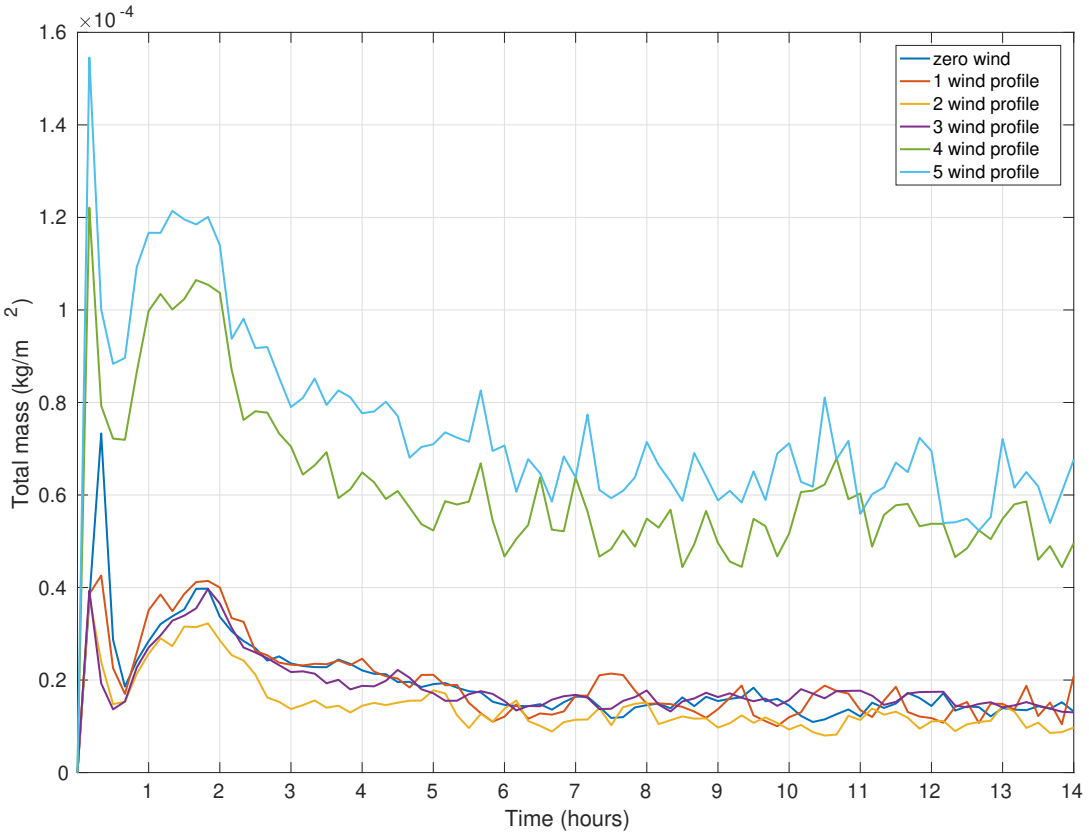

(a)

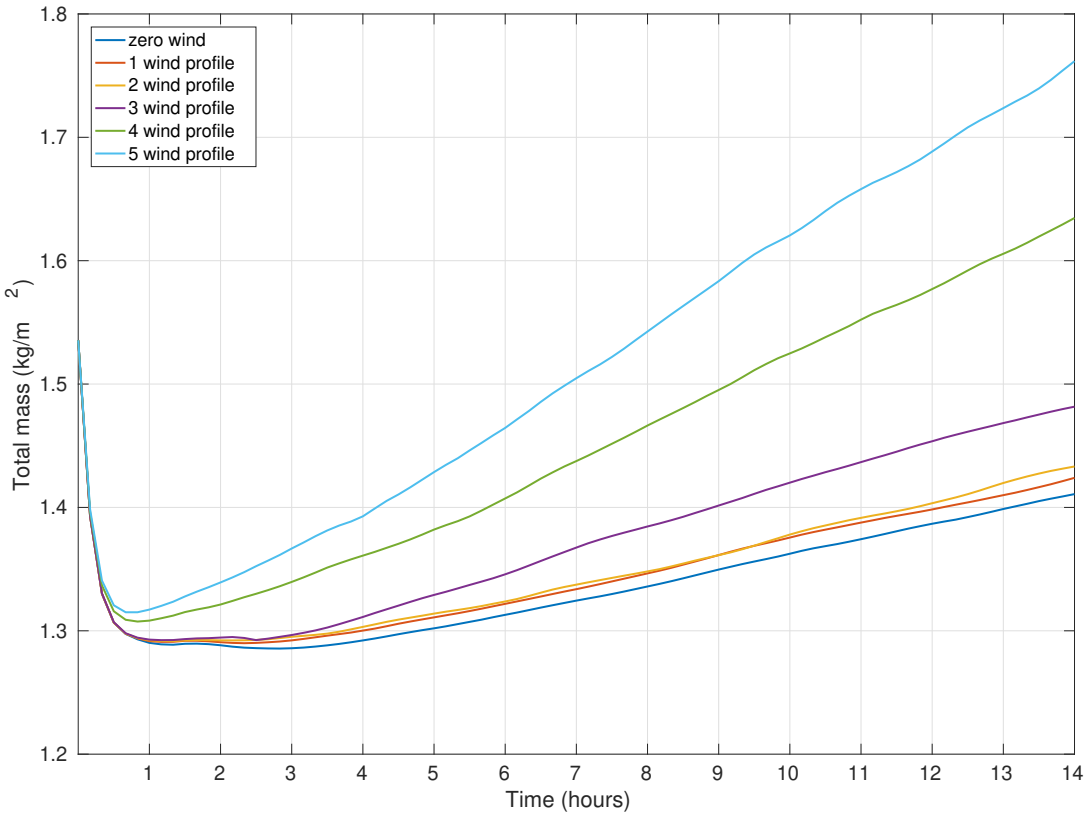

(b)

Supplementary Figure 13: (a) Cloud liquid water total mass for ice concentration $c = 90\%$ and number of floes $N_f = 50$. (b) Water vapor total mass for ice concentration $c = 50\%$ and number of floes $N_f = 5000$.

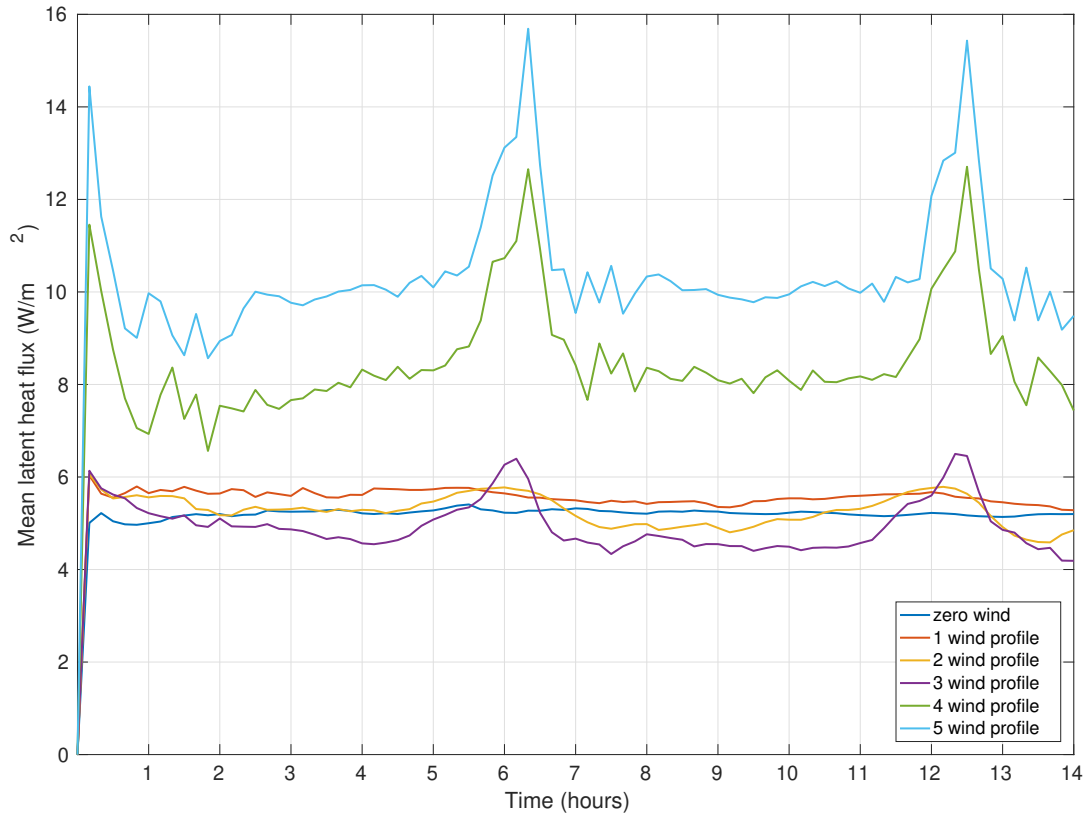

(a)

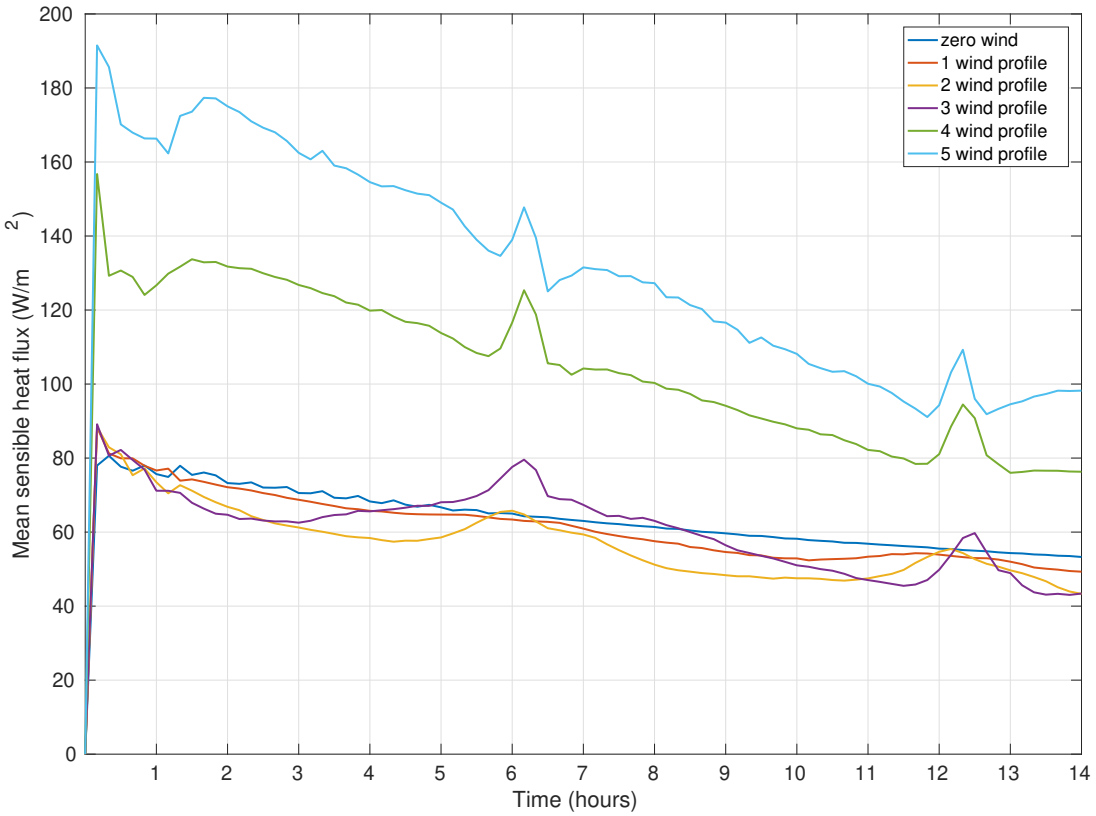

(b)

Supplementary Figure 14: (a) Area averaged latent heat flux, ice concentration $c = 90\%$, number of leads $N_l = 4$ (b) Area averaged sensible heat flux, ice concentration $c = 50\%$, number of leads $N_l = 20$.

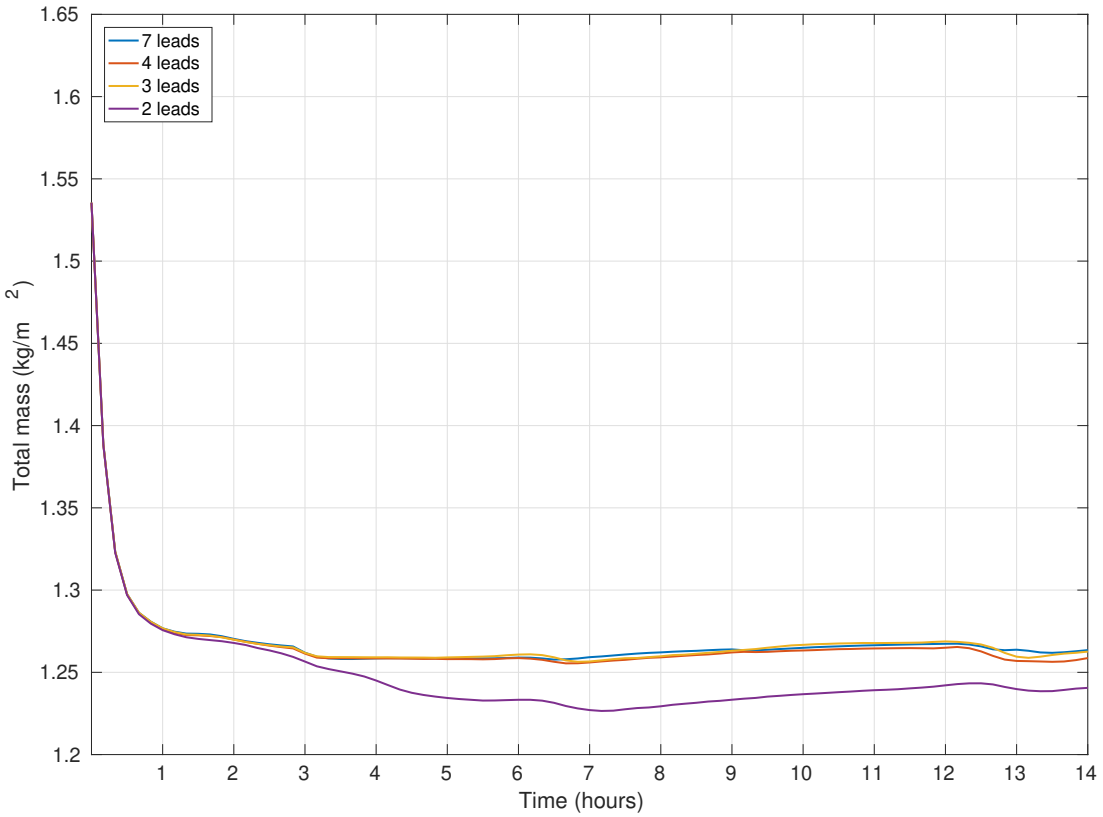

(a)

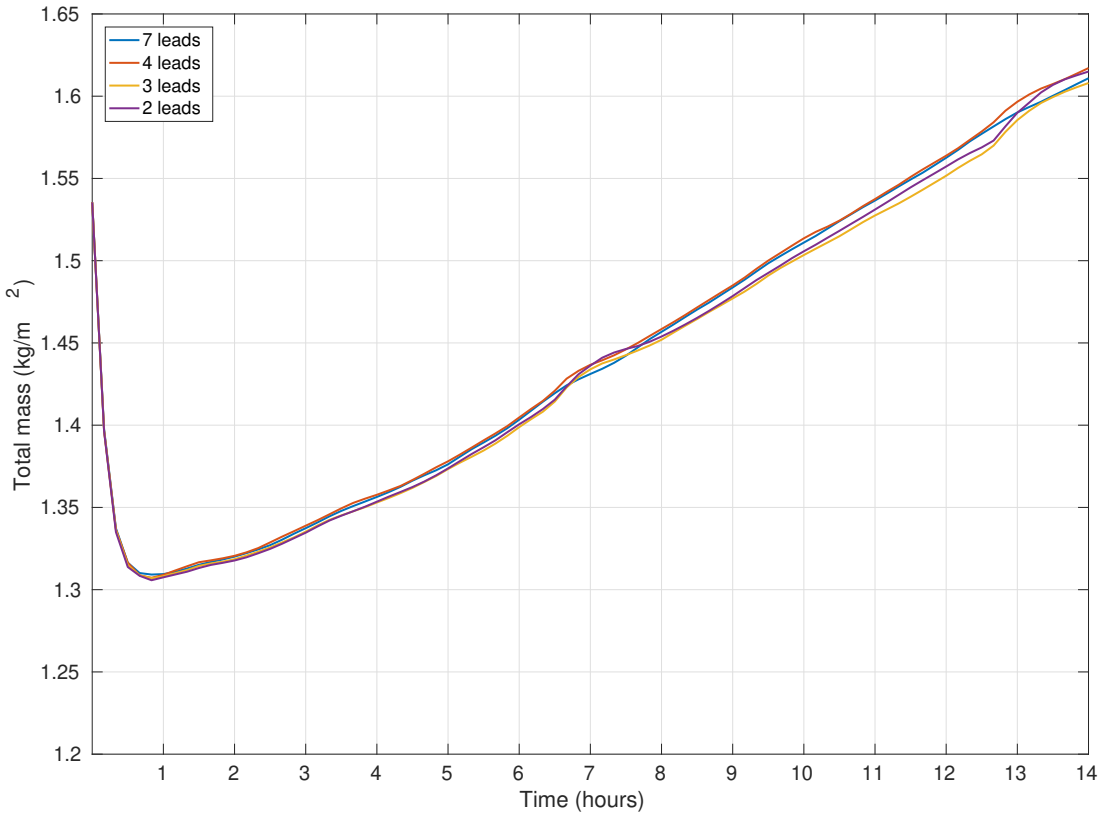

(b)

Supplementary Figure 15: Water vapor total mass for wind profile No. 4 (Fig. 3 in the main text), different leads distributions,(a) ice concentration $c = 90\%$, (b) ice concentration $c = 50\%$.

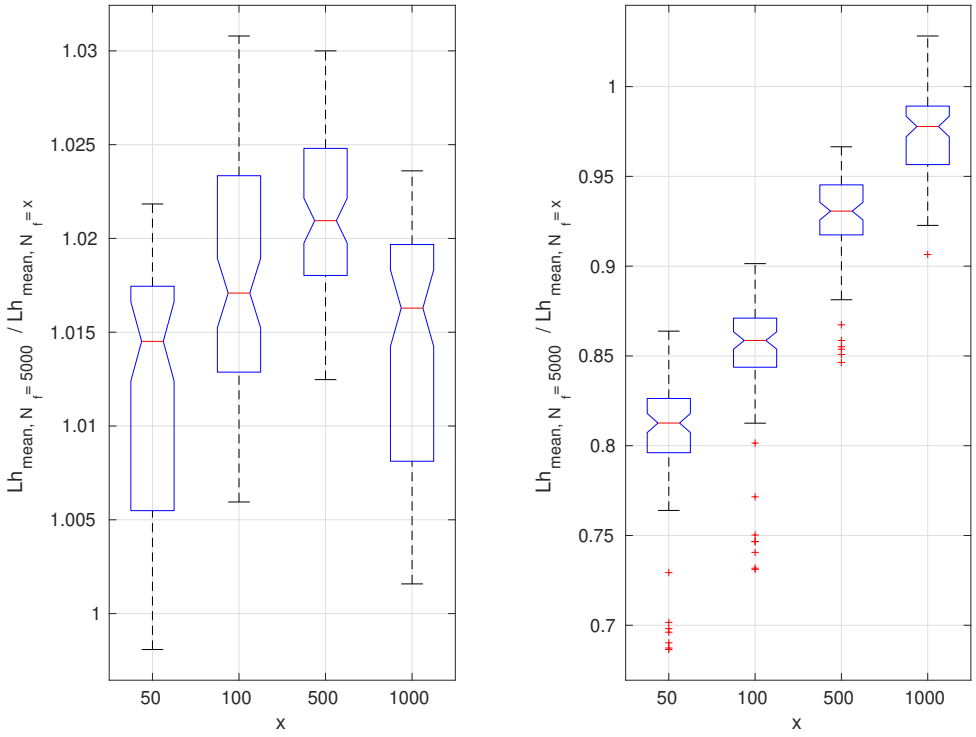

Supplementary Figure 16: Box-and-whisker plots of the results for mean latent heat flux for (a) zero wind simulation and (b) wind profile No. 5 (Fig. 3 in the main text); ice concentration $c = 90\%$, different numbers of floes compared. See Figs. 12 and 13 in the main text for similar plots for $Q_{c,tot}$.

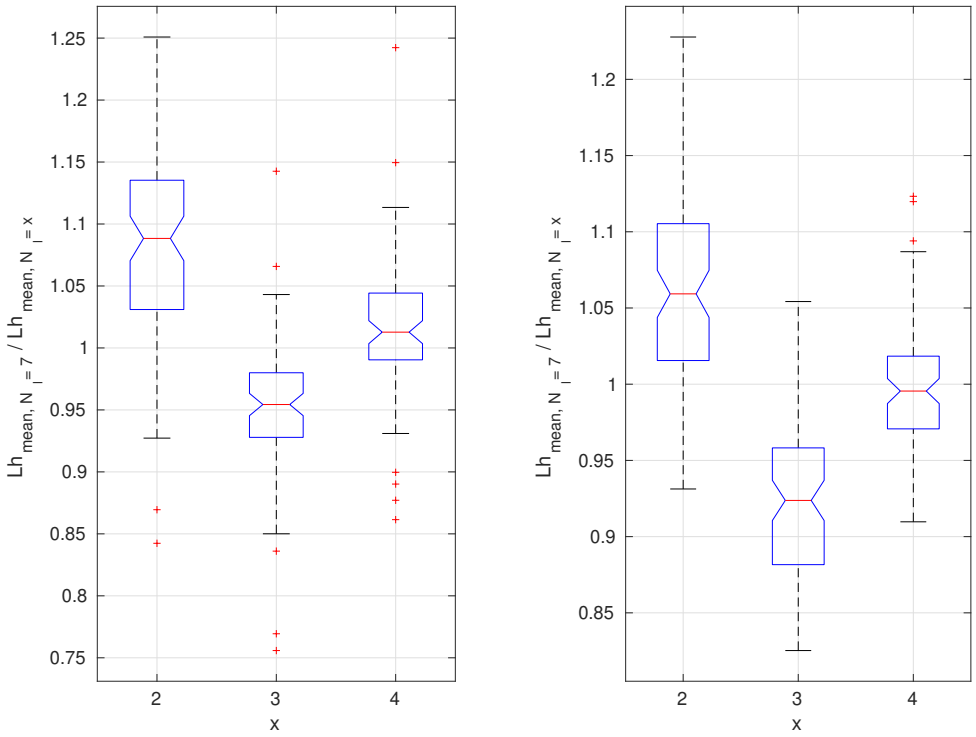

Supplementary Figure 17: Box-and-whisker plots of the results for mean latent heat flux for (a) wind profile No. 4 (b) wind profile No. 3 (Fig. 3 in the main text); ice concentration $c = 90\%$, different numbers of leads compared.

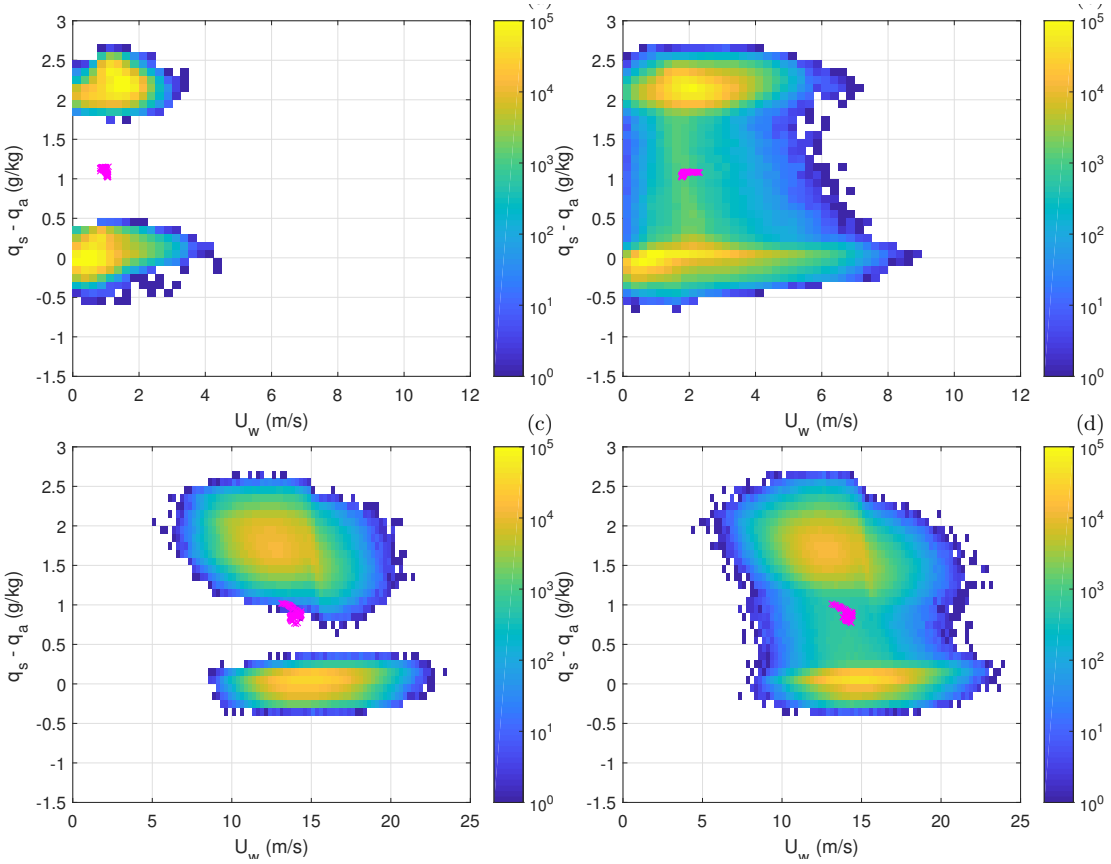

Supplementary Figure 18: Histograms of wind speed U_w and surface–air mixing ratio difference $(q_s - q_a)$ for four selected cases with $c = 0.5$, (a,c): leads, $N_l = 11$; (b,d): round floes, $N_f = 50$; without wind (a,b) and wind profile No. 5 (c,d). Each histogram is based on data from all grid points and times for which results were saved (i.e., every 10 minutes). Bin widths equal 0.25 m/s and 0.1 g/kg, respectively, and the color scale, showing the number of data points within each bin, is logarithmic. Bins without data points are white. Magenta crosses show combinations of area-averaged values ($\langle U_w \rangle$ *versus* $\langle q_s - q_a \rangle$) throughout each simulation. See Fig. 14 in the main text for analogous histograms of U_w and $T_s - T_a$.

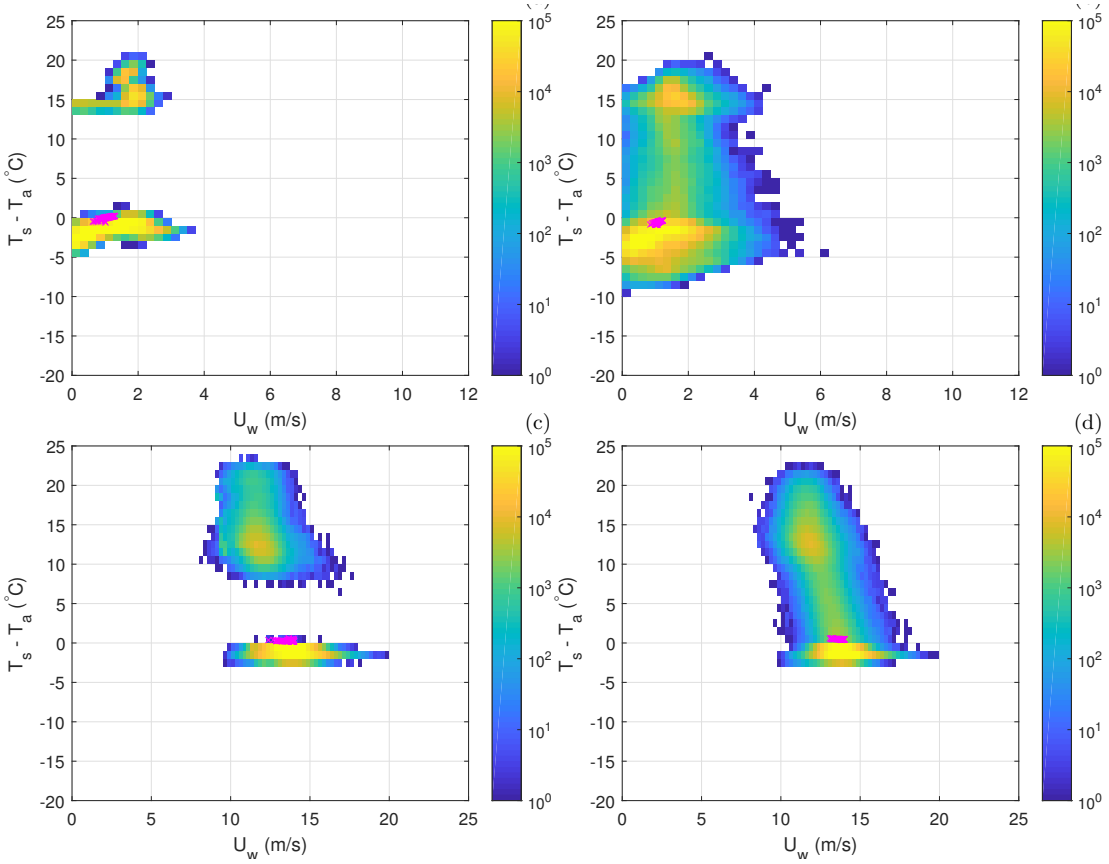

Supplementary Figure 19: As in Supplementary Fig. 18
, but for U_w *versus* $(T_s - T_a)$ and for ice concentration $c = 0.9$.

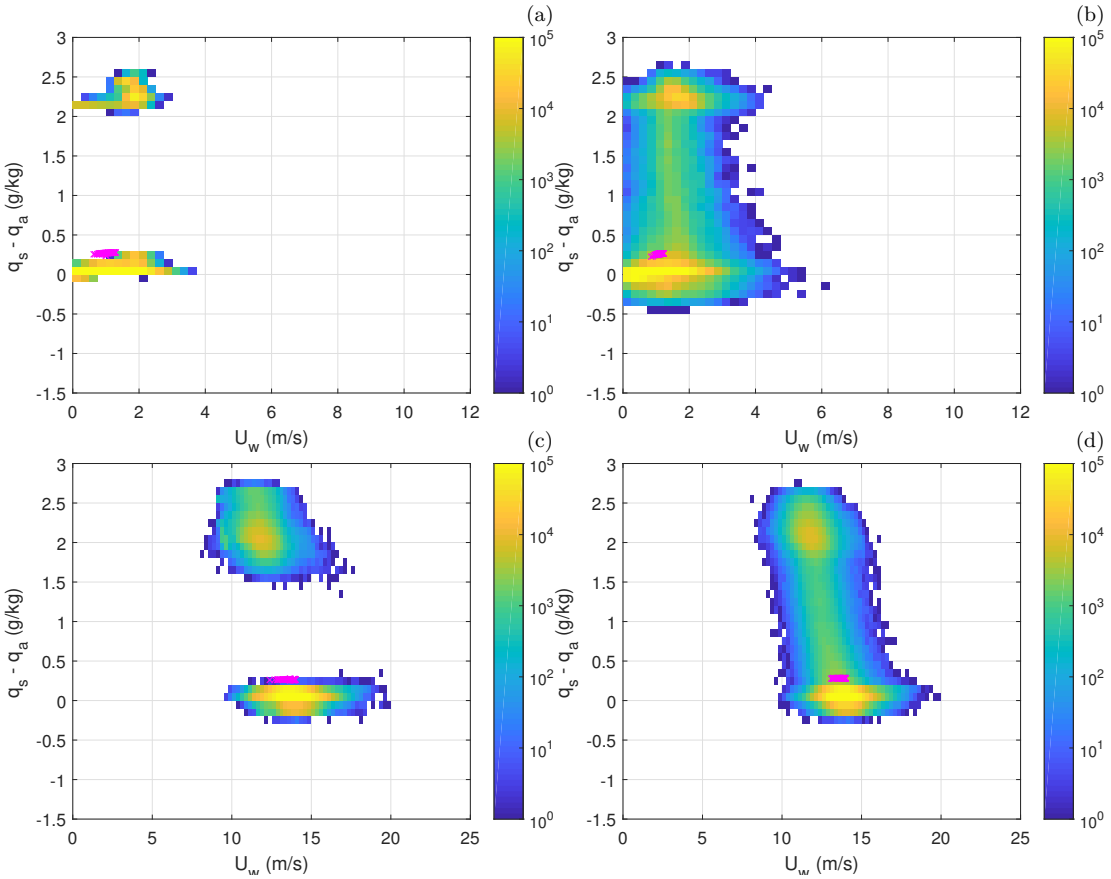

Supplementary Figure 20: As in Supplementary Fig. 18, but for ice concentration $c = 0.9$.

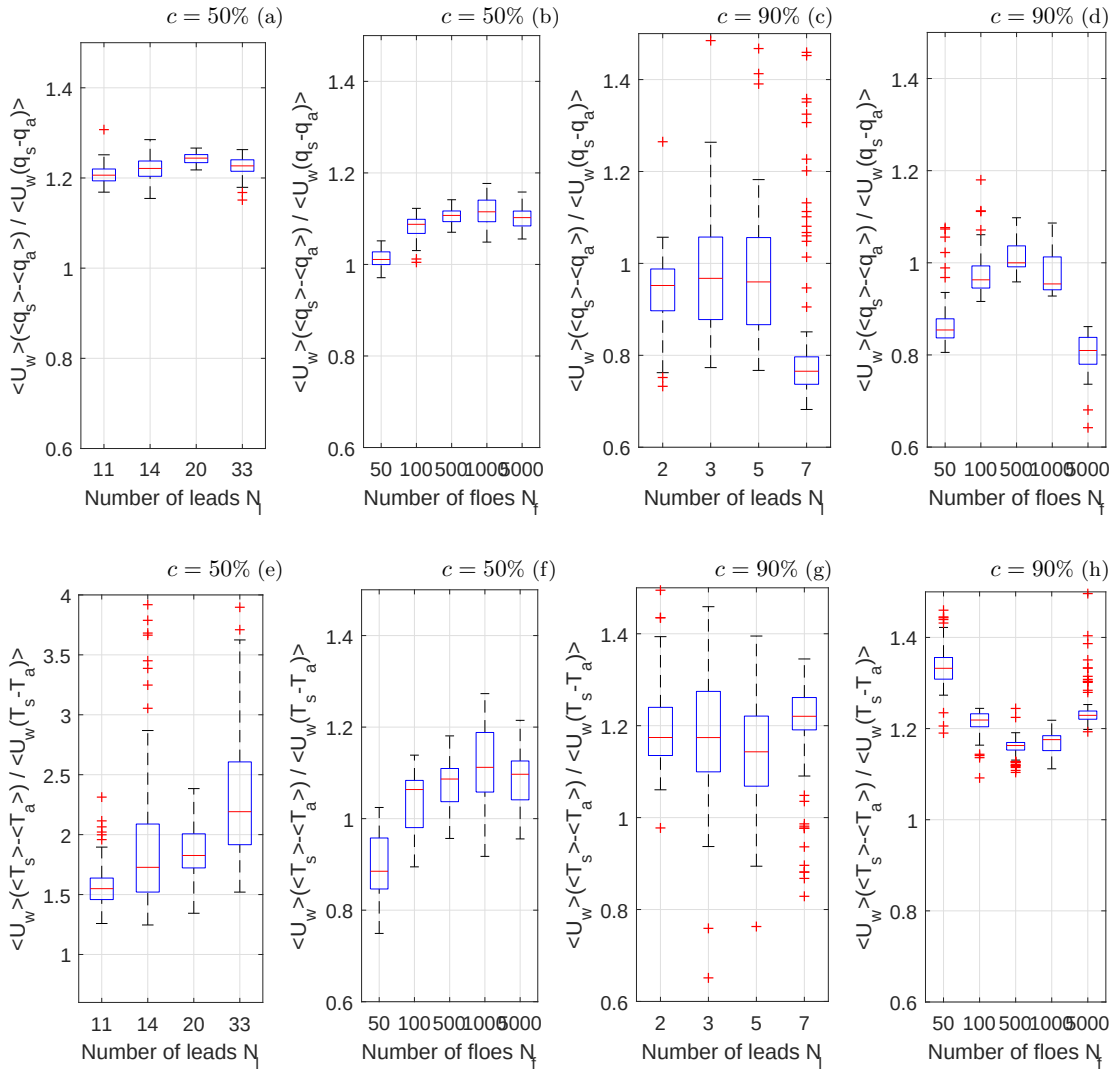

Supplementary Figure 21: Box-and-whisker plots of the ratio α_l (a–d) and α_s (e–h) in simulations with leads (a,c,e,g) and round floes (b,d,f,h) without ambient wind. The ice concentration is written above each plot. Each box shows the interquartile range (blue rectangle) and median (red line), outliers are marked with red crosses.

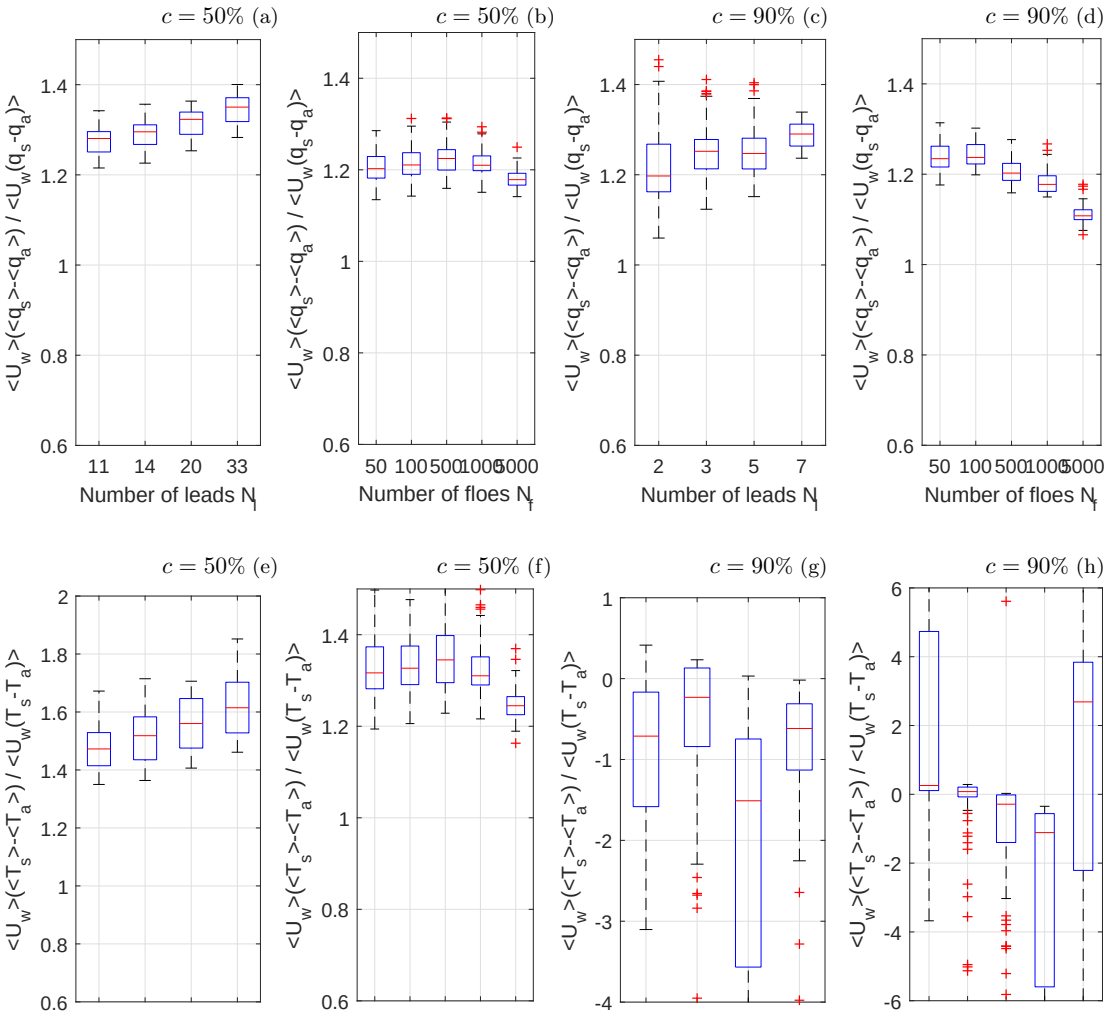

Supplementary Figure 22: As in Supplementary Fig. 21, but for wind profile No. 2.